



Evaluation of methods for measuring tool-chip contact length in wet machining using different approaches (microtextured tool, in-situ visualization and restricted contact tool)

Lars Ellersiek¹ · Christian Menze² · Florian Sauer³ · Berend Denkena¹ · Hans-Christian Möhring² · Volker Schulze³

Received: 23 December 2021 / Accepted: 21 March 2022
© The Author(s) 2022

Abstract

The contact length is one of the most important factors to evaluate the chip formation process and the mechanical loads in metal cutting. Over the years, several methods to identify the contact length were developed. However, especially for wet cutting processes the determination of the contact length is still challenging. In this paper, three methods to identify the contact length for dry and wet processes in cutting of Ti6Al4V and AISI4140+QT are presented, discussed and analyzed. The first approach uses tools with a microtextured rake face. By evaluating the microstructures on the chip, a new method to identify the contact length is established. The second approach applies high speed recordings to identify the contact length. The challenge is thereby the application of high-speed recordings under wet conditions. In the third approach, tools with restricted contact length are used. It is shown that with all three methods the contact length is reduced using metal working fluid.

Keywords Cutting · Lubrication · Contact length · Tool-chip contact · Textured tool

1 Introduction

Metal cutting with a defined cutting edge is one of the most common processes for creating a wide variety of products. The cutting process is characterised by different physical parameters. The main physical characteristics are the thermo-mechanical properties of the process, such as forces and temperatures, as well as the chip morphology and the chip compression ratio. Besides these characteristics, the contact conditions between tool, chip and workpiece are an essential part of a specific cutting process. An important contact criterion between the rake face of the tool and the chip is the contact length. The contact length is significantly involved in the interactions in the secondary cutting zone

and thus influences, e.g., the friction [1] and the heat transfer [2] between tool and chip. The contact zone between the chip and the tool is characterized by two different contact mechanisms: the sticking and sliding area [3]. Each of these areas has a different friction behavior [4–6]. Kato et al. [7], Childs et al. [8], and others measured the tangential and normal stresses by using a split cutter. Zorev proposed a model for the distribution of the tangential and normal stress on the rake face [9]. The model states that the tangential stresses are constant in the sticking area and exponentially decreasing in the sliding area. One possible explanation for the formation of a sticking and a sliding area with different stress characteristics is the real contact area between chip and rake face. The real contact area A_r usually differs from the apparent contact area A_p . Finnie and Shaw proposed a relation between those two areas with:

$$A_r = A_p(1 - e^{-B\sigma_n}),$$

where B is a constant and σ_n the normal load [10]. For high normal loads the apparent contact area A_p approaches A_r . Especially the zone, where $A_p \approx A_r$, is of interest, since there is a high optimization potential due to high contact area and stresses, e.g. by using microtextured tools [11].

✉ Lars Ellersiek
ellersiek@ifw.uni-hannover.de

¹ Institute of Production Engineering and Machine Tools, Leibniz University Hannover, An der Universität 2, 30823 Garbsen, Germany

² Institute for Machine Tools, University of Stuttgart, Holzgartenstrasse 17, 70174 Stuttgart, Germany

³ Institute of Production Science, Karlsruhe Institute of Technology, 76131 Karlsruhe, Germany

The length of the chip-tool interaction in the direction of flow is called the natural contact length [12]. The natural contact length has a complex relationship with the parameters and conditions of the cutting process. For example, different material pairs [13], process parameters [14], chip breakers [15] but also the use of metalworking fluid [16] influence the contact length.

The estimation respectively determination of the natural contact length is possible by analytical, empirical or numerical methods. Lee and Shaffer [17] developed a method of analyzing stress and strain distributions in the plane plastic flow of an ideally plastic material applied to the problem of machining. They derived an equation for the determination of the natural contact length considering the uncut chip thickness, the shear angle and the rake angle. Toropov and Ko [18] presented a new slip line model to determine tool-chip contact length and compared it experimentally with A6061, Copper, SM45C and STS304. The comparison showed a remarkable coincidence. Fatima and Mativenga [19] compared 22 analytical models with an experimental measurement of natural contact length. A fundamental distinction is made between purely analytical and empirical-analytical models. It is shown that some models can predict the contact length with a deviation of 10%. However, the authors point out that the models do not include important boundary conditions. The influence of a metalworking fluid is not considered in the models. Moreover, analytical models assume a continuous chip formation. For materials with a discontinuous chip formation characteristic, no analytical models exist.

Experimental investigations are another possible way to determine the natural contact length. These are often described in the literature in connection with tribological investigations to determine the friction, the contact stresses, and the wear. Several works determine the contact length by examining the contact marks on the rake face using a scanning electron microscope [3, 14]. Friedman and Lenz [20] summarized the effect of an artificially controlled contact length. According to them, a decreasing contact length leads to decreasing normal and tangential forces. The relationship is usually linear. Investigations of Heisel et al. [21] showed that the forces and the chip compression ratio decrease if the rake face falls below the natural contact length. Thus, the point of falling forces can be used to determine the natural contact length. Ortiz-de-Zarate et al. [22] similarly investigate the contact conditions in the machining process using a special tool with a groove. Bergman and Grove used high-speed recordings of the cutting process to identify the contact length [23].

Most of the investigations presented in the literature are carried out under dry conditions. However, the use of a metalworking fluid has a significant influence on the machining process. In addition to the transport function,

the metalworking fluid influences the thermomechanical and tribological characteristics of the process. De Chiffre [24] explained that metalworking fluids have often a very strong influence on the cutting process in reducing forces, chip compression etc. However, the mechanism by which this happens has long been a controversial topic. Three main schools for lubrication in cutting exist. The first theory states, that by using lubrication a soft film between tool and chip is present. A second approach proposes that in a physiochemical reduction of the work material shear strength. The last theory is the reduction of contact between the tool and chip. In Ref. [25] De Chiffre showed in his experiments that the use of a cutting oil or emulsion leads to a reduction in the natural contact length. More recent work such as by Varadarajan et al. [26] and Dixit et al. [27] demonstrate the same behavior using minimum quantity lubrication (MQL). This review of the literature shows the historical development and the importance of the contact length in the characterization of a specific metal cutting process and the resulting contact stresses. However, most of the work relates to investigations of the contact length under dry cutting conditions. This paper establishes and compares three different methods, to estimate the contact length in wet machining. The first method utilizes microtextured tools to identify the contact length. A comparatively new area of machining science is the study of structured and textured cutting tools. A comprehensive overview is given by Özel et al. [28]. This field offers new possibilities for investigating the mechanisms in the contact area between chip and tool during the cutting process and can serve as an alternative to existing methods such as restricted tools or video kinematic observations with high-speed recordings. Microstructures applied in machining have to this date only been considered in research regarding minimizing friction and process forces [29, 30]. A mapping of the inverse patterns of the laser textures on the back of the chip has not yet been considered in order to determine the contact length cl in the cutting process. Investigations by Patel et al. showed in 3D chip formation simulations that an applied laser texturing on the simulated tool can be detected in the chip surface, but this finding was not used to further investigate the contact length [29]. Therefore, the application of microtextured tools to measure the contact length represents a novel and innovative approach. The second approach uses high speed recordings to determine the contact length. While high speed recordings are commonly used in dry cutting processes, the application in wet processes represents a novel method and is challenging because of the limited visibility of the cutting process in wet machining. The third approach is the restricted contact length. This well-established method is widely used in the study of contact mechanisms between chip and tool and was already applied in wet machining processes. Finally, the three methods are compared and an overview of advantages and disadvantages

for the different methods applied in wet machining, which is currently not available in literature, is given.

2 Experimental procedure and methodology

2.1 Investigations with laser textured tools

The first approach investigates the tool-chip-contact length with micro-textured cutting tools. Therefore, orthogonal turning tests were accomplished with a CNC vertical turning machine of type Index V100 (Fig. 1). In order to investigate the influence of cooling on the contact length of the chip to the rake face, the tests were carried out in dry and wet cutting with a water-based metalworking fluid, which was applied directly to the rake face with a pressure of 6 bar. The specimen material used was AISI 4140+QT ($R_m=974$ MPa, Hardness HV0.1 360, heat treatment according to ISO 683-18) and Ti6Al4V ($R_m=954$ MPa) with a diameter of 48 mm. In the experiments, 1 mm of the diameter was machined in each case. While the uncut chip width of the steel specimens was $b=4$ mm the titanium tests were carried out with $b=3$ mm, since the cutting forces are expected to be higher than those of steel.

Coated carbide tool inserts of the type CCMW120404-06 with a rake angle of $\gamma=0^\circ$, a clearance angle of $\alpha=7^\circ$ and a cutting edge rounding of $30\ \mu\text{m}$ without chip breaker were used for the tests. These cutting tools are coated with

an AlCrN-layer by Oerlicon Balzers. Additionally, the cutting inserts were modified with a microstructure on the rake face (Fig. 2), which was applied by laser ablation with a TRUMPF TruMicron 5050. The micro-textures are applied in the direction of chip flow on the rake face of the insert and have a depth of $7\ \mu\text{m}$ and width of $50\ \mu\text{m}$. The individual textures have a spacing of $100\ \mu\text{m}$. The first micro-texturing is $210\ \mu\text{m}$ away from the cutting edge. This means that only contact lengths above this distance can be detected. To determine the contact length in the orthogonal cut, the laser textures are applied at a steady increasing angle, which means that in the y-direction the textures are located $10\ \mu\text{m}$ further away from the cutting edge. It is expected that this laser structure will be embossed to the chip surface during the tests and thus the contact length of the chip can be determined using a confocal microscope of the type nanofocus MarSurf CP.

In order to enable a comparison of the tests carried out with different machines and coatings, the cutting parameters described in the following sections were set to a cutting speed of 120 m/min and an uncut chip thickness of 0.1 mm for AISI 4140. In addition, for AISI 4140, also the cutting depth of 0.15 mm and, for titanium, the cutting depths of 0.2 mm and 0.25 mm were investigated in the tests. The experiments were performed once for each of the two approaches. Subsequently, the resulting undersides of the chips at three different locations, beginning, middle and end of the cut, were analysed by means of topography images in order to obtain a statistical validation.

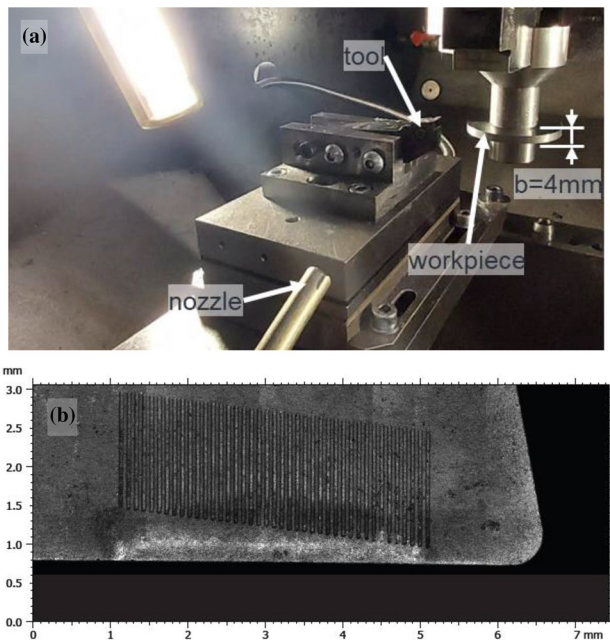


Fig. 1 a Experimental setup for orthogonal turning with micro textured cutting inserts, b Microstructures on rake face

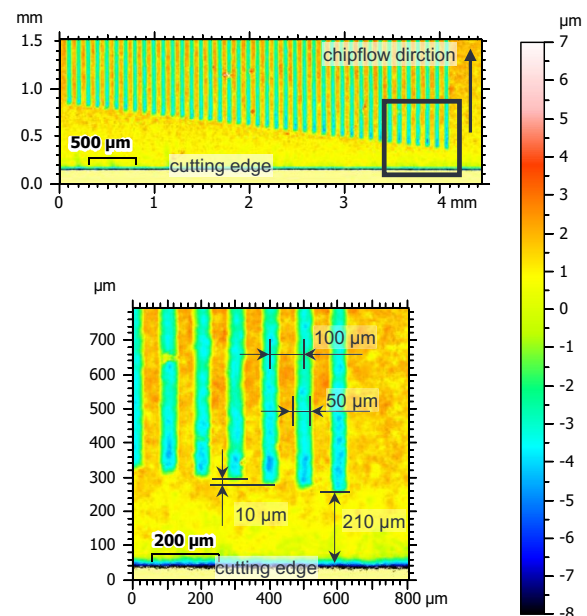


Fig. 2 Topography images of the micro texturing on the rake face of the insert used

The novelty of this method lies in the fact in the current state of research. The contact lengths have not been investigated so far via microtextured cutting inserts. The method thus represents a new and alternative method compared to the established ones.

2.2 Investigations with high-speed recordings

The second approach investigated in this paper is the high-speed recording of cutting processes. Thereby, a planing test rig was used. The cutting process was recorded using a high-speed camera Photron Fastcam SA5 and a SMETec LED-P40 light source. The videos were recorded with a framerate of 20,000 fps, a shutter of 1/106,000 and a 6× magnification. In addition, a dynamometer Kistler 9257B was used to measure the process forces. The pixel size is $3.3 \mu\text{m} \times 3.3 \mu\text{m}$, which is 1.2% of the lowest contact length identified at uncut chip thickness $h = 0.1 \text{ mm}$. To enable processes with metalworking fluid, the planing test rig was extended (Fig. 3). A housing was added to the table of the planing test rig to protect the machine components and the high speed camera. The housing has a recession at the workpiece, where a sapphire glass is placed to allow high-speed recordings of the cutting process. Furthermore, the holder of the metalworking fluid nozzle provides additional protection against the metalworking fluid. The high-pressure cooling is realized by an accumulator. The accumulator is pre-charged with the metalworking fluid with a defined pressure and the valve of the accumulator is opened using a relay-card shortly before the cutting process begins. A detailed description of the extended test rig is given in [31].

In the investigations, AISI4140 + QT was machined. The same heat treatment according to ISO 683-18 was used as in the investigations with structured tools. Vickers hardness was measured with a mean value of 393 HV1 (10 measurements on different positions, min 375 HV1, max 411 HV1). The slight differences in hardness compared to the workpiece in Sect. 2.1 can be attributed to the different dimensions of the workpieces. The maximum uncut chip thickness was $h_{\text{max}} = 0.1 \text{ mm}$ and the uncut chip width $b = 2 \text{ mm}$.

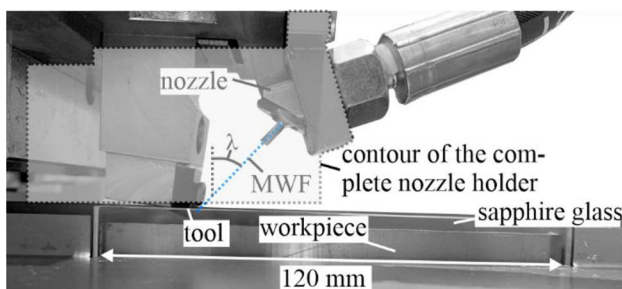


Fig. 3 Extended planing test rig for experiments with high pressure metalworking fluid [31]

On the first 33 mm of the workpiece, the uncut chip thickness increased linearly from 0 to 0.1 mm. This enables the knowledge about the influence of the uncut chip thickness on contact lengths and process forces. All investigations were conducted with a constant cutting speed $v_c = 120 \text{ m/min}$. The used cemented carbide tools from Kennametal (SNMA120408 K68) had a rake angle $\gamma = 1^\circ$ and a clearance angle $\alpha = 14^\circ$ and were coated with a TiAlN coating. The rake face of the tool was polished before the coating process. The cutting edge rounding was chosen with $S_\alpha = S_\gamma = 35 \mu\text{m}$, which is typical for machining of steel [32]. Cutting tests were performed with three different cooling strategies (dry, $p = 10 \text{ bar}$, $p = 30 \text{ bar}$). A 10% emulsion Zeller + Gmelin Zubora 67H Extra was used as metalworking fluid.

The novelty of this approach lies in the implementation high-speed recordings on a wet cutting process at a microscopic scale.

2.3 Investigations with restricted contact tools

In addition to the approaches already presented, a restricted contact length method is used for the investigation of Ti6Al4V. The approach can be used for dry and wet cutting. The basic idea is related to the decreasing cutting force characteristic with restricted chip-tool contact length. The cutting forces measured on the tool result from the complex tool-chip interactions that occur in the forming and friction process. If the length of the rake face decreases below the natural contact length, the chip-tool interaction is shortened, and the cutting forces decrease [8, 20]. This effect can be used to estimate the natural contact length [21, 22]. To investigate the influence of a metalworking fluid on the natural contact length during the machining of Ti6Al4V, in this paper cutting tests were carried out to determine the cutting and cutting normal force with a prepared tool with a defined rake face length. At the beginning of the tests, the rake face length must be longer than the natural contact length. In the following, the contact length is continuously shortened and the cutting and cutting normal force are measured in relation to each contact length. If the rake surface finally is shorter than the natural contact length, a decrease in force can be seen in comparison to the forces already measured. The point at which the forces fall indicates the natural contact length. In the following, the experimental investigation of the influence of a metalworking fluid on the natural contact length and the resulting normal and shear stress for the material Ti6Al4V is presented. Ti6Al4V has a discontinuous chip formation characteristic in the considered parameter range. Consequently, the chip formation is characterized by a time-dependent stagnation and shear phase. Therefore, the averaged forces are considered in the following. This influences the calculation of the stresses since the calculated figures

correspond to an average value. The natural contact length can nevertheless be determined with an adequate confidence.

The experiments were carried out on a turning machine of the type GILDEMEISTER CTX 420 linear. The tools used are carbide inserts from Sandvik-Coromant (SNMA 15 06 12-KR 3225). These inserts have a neutral rake and flank surface with no chip breakers. For the cutting experiments quasi-orthogonal turning with a workpiece diameter of 80 mm was used (Fig. 4). The forces were measured by a Kistler dynamometer Type 9121. In the investigation annealed Ti6Al4V was machined ($R_m \geq 895$ MPa, Hardness ≤ 310 HB). The Metalworking fluid was implemented by a nozzle near the cutting zone. The metalworking fluid used was a water-based emulsion Blaser Blasocut BC935 Kombi with 8% concentration. The pressure of the metalworking fluid was set to $p=30$ bar.

The experiments were executed according to the procedure shown in Figs. 4 and 5. First, the tools were prepared for

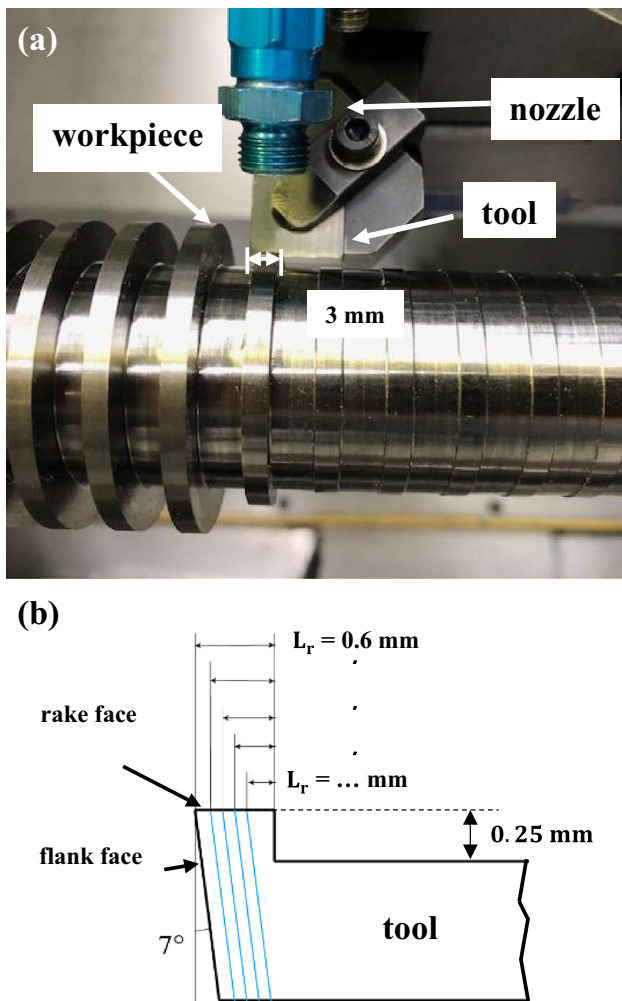


Fig. 4 a Experimental setup of quasi-orthogonal turning; b Preparation of restricted tools for the cutting experiments

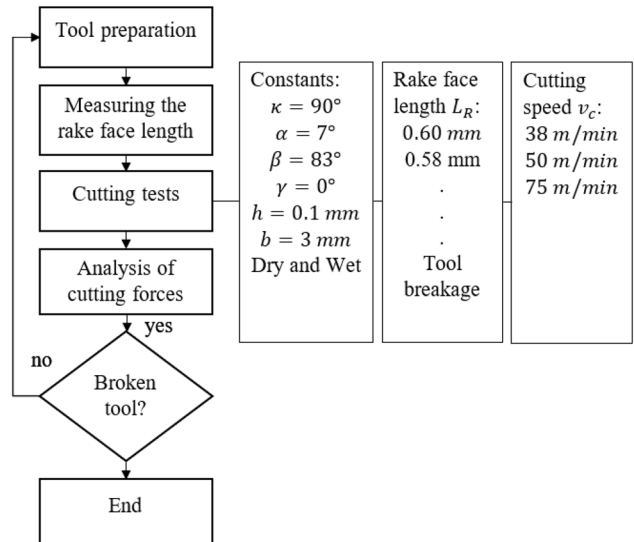


Fig. 5 Experimental procedure and settings

the experiments. Initially, the rake face is reduced by 0.5 mm to create a defined rake face length. In the next step, the clearance face of the insert is ground back at an angle of 7° in the tool holder on a grinding machine. Thereby, a defined rake face length of $L_r=0.60$ mm is achieved (Fig. 4b). The cutting edge rounding was chosen to $S_\alpha=S_\gamma=20$ μ m and prepared after grinding using a brushing process. After the rake face and the cutting edge rounding has been measured, cutting tests can be carried out. Figure 5 illustrates the experimental settings of the investigation. This includes the constant geometric parameters such as the cutting edge angle κ , the clearance angle α , the wedge angle β and the rake angle γ . The process conditions include a chip width $b=3$ mm, an uncut chip thickness $h=0.1$ mm and 1 mm of the diameter was machined. The experiments start with a rake face length of $L_r=0.60$ mm. In the following, the rake face length is successively shortened in steps of 20 μ m according to Fig. 4b. For each rake face length, three different cutting speeds, each dry and wet, with three repetitions were carried out. The experiments end with the tool breakage.

3 Results and discussion

3.1 Investigations with laser textured tools

The contact lengths in machining with modified micro textured inserts for the materials AISI 4140 and Ti6Al4V were investigated under dry and wet ($p=6$ bar) machining. Results of the investigated uncut chip thickness of 0.15 mm for AISI 4140 are shown in Fig. 6 as a topographical image of the back of the chip. For the investigation of

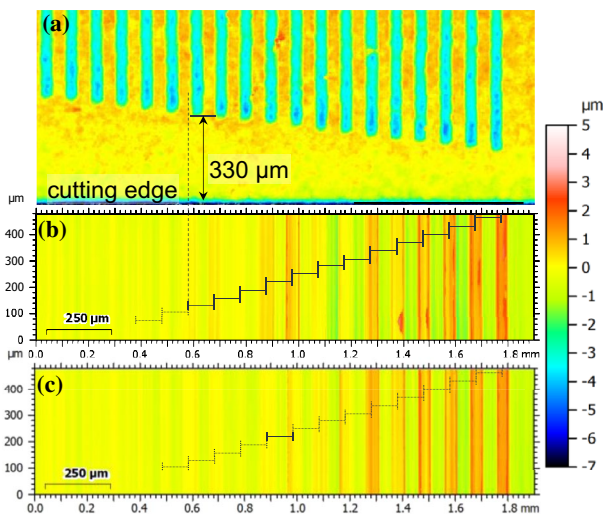


Fig. 6 **a** Topographical image of macrotextured rake face. **b, c** Topography images of the inverse microtexturing on the back of the chip for AISI4140 and an uncut chip thickness of $h=0.15$ mm and $v_c=120$ m/min. **a** Dry machining $l_c=330$ μm , **b** wet machining $l_c=300$ μm

the dry (Fig. 6b) and wet (Fig. 6c) test results, the inverse microtextures on the chip can be clearly identified. For this purpose, the distance of the start of microtexturing on the cutting insert was identified as the minimum detectable contact length. By counting the inverse microtextures on the chip surface, by means of topographical images the determined contact lengths between the chip and the rake face is detected. This results in a total contact length of 330 μm for the tests carried out without metalworking fluid and 300 μm for the wet experiments (black lines in the distance of the textures). As shown in Fig. 6, the contact length cannot be determined unambiguously, since individual lines of microtexturing can still be detected slightly (height > 1 μm , dotted lines). For a clear classification of the contact length, the threshold of > 1 μm is used. The inverse textures that are below this limit are marked as uncertainty. If this finding is taken into account, the contact length of the dry experiments can be determined to be 350 μm and the wet experiments to be 340 μm due to the uncertainty in chip formation. However, what can be clearly observed is that the contact length decreases under the use of metalworking fluid, this finding coincides with those of the Sects. 3.2 and 3.3.

The same results can be observed for the experiments carried out for Ti6Al4V. The inverse texturing on the backside of the chip could only be detected at a chip thickness of 0.2 mm. Tests carried out below this chip thickness did not lead to clear results. The results for the uncut chip thickness 0.2 mm are shown in Fig. 7. The backside of the chip for Ti6Al4V is shown for dry (Fig. 7b) and wet (Fig. 7c) machining. Since the contact length is not

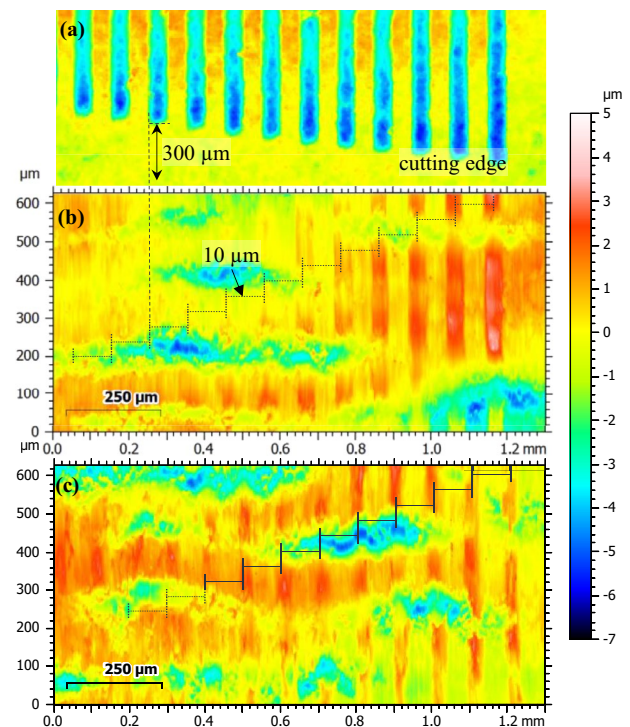


Fig. 7 Topography images of the inverse microtexturing on the backside of the chip for Ti6Al4V and an uncut chip thickness of $h=0.2$ mm and $v_c=120$ m/min. **a** Dry machining $l_c=300$ μm **b** wet machining $l_c=290$ μm

continuous when machining Ti6Al4V, only the maximum effective contact length can be determined by this method. For the dry tests, a minimum contact length of 300 μm can be clearly determined. With the inclusion of the uncertainty, a maximum contact length of 320 μm appears. As in the tests with the material AISI4140, a reduction of the contact length to a minimum of 290 μm and with uncertainty to a maximum of 310 μm can be observed for wet cutting. This difference is much smaller than in the tests with AISI4140.

The results of the tested uncut chip thicknesses for the materials AISI4140 and Ti6Al4V are shown in Fig. 8. The dry tests are shown in blue and the wet tests in red. Furthermore, the observed uncertainty is quantified by the shaded bars. It can be generally stated that the contact length is reduced by the use of metalworking fluid for both materials in the orthogonal cut. However, for the tests of Ti6Al4V, a significant influence can only be determined at higher chip thicknesses, through the use of micro textured tools. This can be attributed to higher normal stresses and the associated higher local pressures. Due to these local pressures, the laser texturing can be better transferred to the surface of the chip. Furthermore, it can be said that for the test material Ti6Al4V the contact length measured with the method presented is only slightly influenced by the use of metalworking fluid.

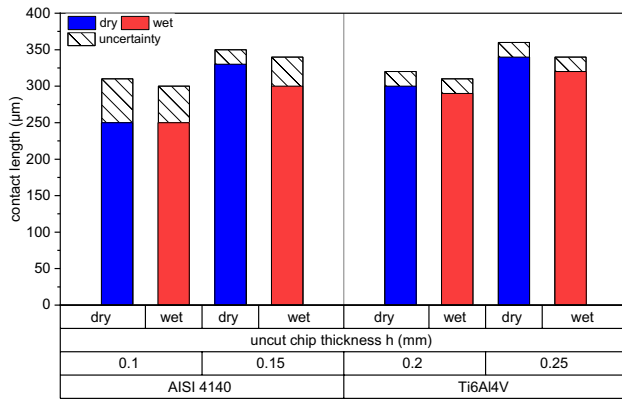


Fig. 8 Results of contact length measurement for AISI4140 and Ti6Al4V at cutting speed $v_c = 120$ m/min dry and wet (mean value of three measurements on different positions)

It has to be mentioned that the micro-texture can influence friction and contact conditions between tool and chip [28]. Therefore, further methods to identify the contact length are used in the following to validate the results.

In the contact length study with laser textured inserts, the ratio of A_r/A_p is close to 1, which means that the measured results are in agreement with the real contact zone near the cutting edge at high plastic deformation.

3.2 Investigations with high-speed recordings

High speed recordings of orthogonal cutting of quenched and tempered AISI4140 were conducted without metalworking fluid and with metalworking fluid pressures $p = 10$ bar and $p = 30$ bar. Images of the cutting process when reaching the maximum uncut chip thickness of $h = 0.1$ mm are given in Fig. 9. For the dry cutting process, a continuous chip formation with a defined contact length $cl = 0.49$ mm is visible (Fig. 9a). By applying metalworking fluid with a pressure $p = 10$ bar, metalworking fluid is present on the right hand side of the chip (Fig. 9b). In addition, the metalworking fluid hits the top of the chip and squeezes the chip against the workpiece surface due to the mechanical impact of the metalworking fluid. This effect leads to a reduction of the contact length. However, no penetration of the metalworking fluid in the gap between chip and rake face on the secondary shear zone is visible. This corresponds to findings from literature [1, 24], which indicate that the penetration of the metalworking fluid in the secondary shear zone here is challenging due to the movement of the chip against the penetration direction of the fluid. However, a micro-film formation on the rake face can enhance the lubrication on the rake face even though no macroscopic fluid stream is visible [1, 24].

An increase of the fluid pressure to $p = 30$ bar further decreases the contact length between chip and rake face due to the higher jet forces and the higher flow rate (Fig. 9c).

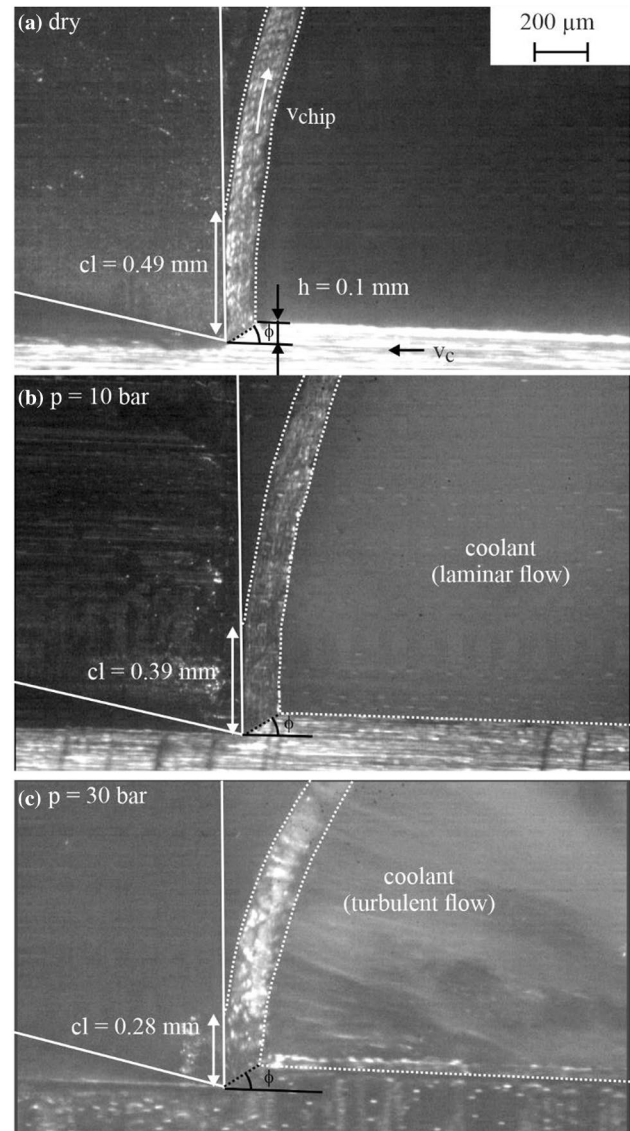


Fig. 9 High speed images of orthogonal cutting of AISI4140+QT with $v_c = 120$ m/min, $h = 0.1$ mm, $b = 2$ mm for different cooling strategies (a dry process, b $p = 10$ bar, c $p = 30$ bar)

Furthermore, it can be seen that the fluid condition on the right hand side of the chip changes from a laminar to a turbulent flow. This can be attributed to the higher fluid velocity, which leads to a higher Reynolds number Re .

Besides the contact length, the shear angle can also be identified on the high speed images. The shear angle is in the range of $\phi = 32\text{--}35^\circ$ for all processes. This indicates only minor changes of the friction due to the metal working fluid, since a reduced friction is associated with an increase of the shear angle. Thus, the tribological conditions only change slightly.

The continuously increasing uncut chip thickness h during the beginning of the process enables a detailed analysis

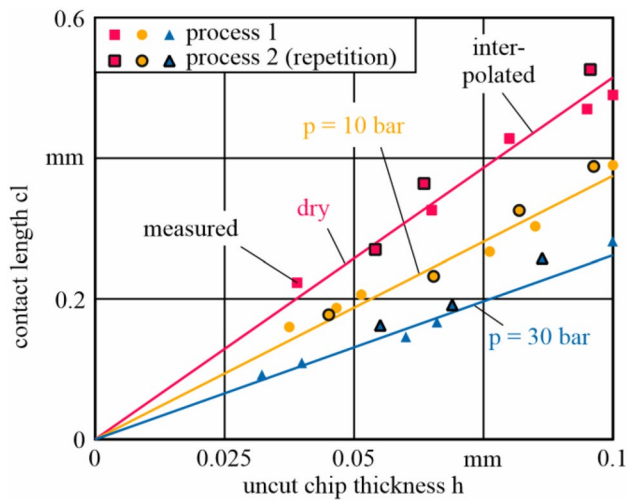


Fig. 10 Influence of uncut chip thickness h on the contact length for different cooling conditions ($v_c=120$ m/min, $b=2$ mm, material: AISI4140+QT, two experiments per cooling strategy)

of the contact length for different cutting conditions. The influence of the uncut chip thickness h on the contact length cl is given in Fig. 10. The contact length is analysed for two experiments per cooling strategy. Due to the observation of the cutting process, possible errors, e.g., an incorrectly set uncut chip thickness, can be detected, which leads to a high repeatability of the method. For all analyzed uncut chip thicknesses, the contact length decreases with increasing metalworking fluid pressure. Moreover, the behavior of the contact length cl in dependence of the uncut chip thickness h can be described as nearly linear for all cooling strategies as shown by interpolated curves in Fig. 10.

Compared to the contact lengths identified with laser prepared tools in Sect. 3.1, the identified contact lengths are increased up to 90%. Even though slight differences in the contact length can be expected using different tool coatings, the different results can mostly be attributed to the peculiarities of the methods. To make this point clear, high speed recordings on the planing test rig were also performed with a laser prepared tool. For those tests, the same cutting parameters as in the previous investigations ($v_c=120$ m/min, $h=0.1$ mm) were used. The rake face and the chip surface of the unprepared reference tool are given in Fig. 11a. Rake face as well as chip have a smooth surface. The structure created on the rake face using pulsed laser ablation is given in Fig. 11b. The structures are clearly visible. The individual grooves have a distance of $80\ \mu\text{m}$. The distance of the grooves to the cutting edge increases by $20\ \mu\text{m}$ for every groove. The depth of the grooves is $10\ \mu\text{m}$. The individual grooves of the laser prepared rake face are visible on the chip surface. However, as with the already presented results, the transition area is not clearly visible, since the interaction between chip surface and the grooves on the rake face

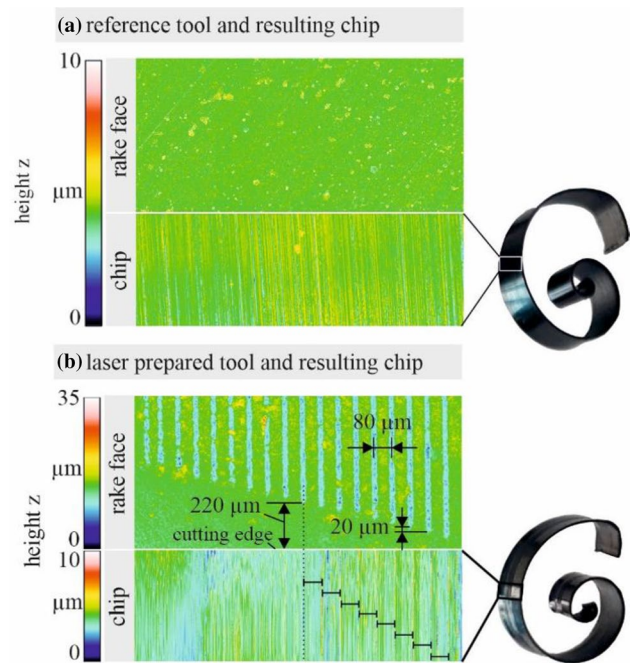


Fig. 11 a Rake face and chip surface of an unprepared reference tool, b laser prepared rake face and resulting chip surface ($v_c=120$ m/min, $h=0.1$ mm, $b=2$ mm, material: AISI4140+QT, lubrication: dry, one experiment per tool)

is only small in this area. By evaluating the chip surface shown in Fig. 11b, a contact with nine grooves is assumed. This results in a contact length of $220\ \mu\text{m}$. This is in good agreement with the contact length for dry machining of AISI4140+QT with $h=0.1$ mm (Fig. 8). Based on the high speed images, however, a contact length of $490\ \mu\text{m}$ (reference tool) and $450\ \mu\text{m}$ (laser prepared tool) were measured. The contact length is therefore only slightly influenced by the grooves on the rake face, indicating that the chip formation process here is only slightly influenced by the rake face. This is also proven by similar chip forms for both processes as shown in Fig. 11. Thus, both methods are in general applicable to qualitatively compare the contact length. The deviations between contact lengths for the two methods ($220\text{--}450\ \mu\text{m}$) can be explained by the stress distribution and the difference between apparent contact area A_p and real contact area A_r on the rake face. As stated before, the apparent contact area A_p identified with the laser textured tool nearly equals the real contact area A_r . The reason for this are the high normal loads near the cutting edge. The apparent contact area between the contact length identified with laser textured tool $cl=220\ \mu\text{m}$ and the contact length identified on high-speed images $cl=450\ \mu\text{m}$, on the other hand, is significantly bigger than the real contact area in this zone. The contact between chip and rake face in this zone continuously decreases with increasing distance from the cutting edge and approaches to zero.

3.3 Investigations with restricted contact tools

The investigations presented so far show methods for determining the contact length by means of optical analysis of the actual process or by evaluating the resulting abrasion effects. The restricted contact length tools method for determining the natural contact length is a force-based analysis of the change in the chip-tool interaction length. If a first drop in force occurs, this indicates that the sliding zone has been reached. If the rake face is shortened further, the tool-chip contact zone is increasingly undercut. Materials such as Ti6Al4V are characterized by a discontinuous chip formation. Thereby, the contact length and the mechanical loads acting on the rake face change continuously even for processes with constant uncut chip thickness. Thus, a clear assignment between uncut chip thickness and contact length as shown in Fig. 9 is not possible. A measurement of the contact length with continuously increasing uncut chip thickness, as shown before (Sect. 3.2), is therefore not reasonable. Instead, measurements under defined process parameters are necessary for an effective evaluation of the chip formation. Since a repetition of planning tests for several different uncut chip thicknesses is associated with a high experimental effort due to the time-consuming alignment of the high-speed camera equipment, the method of restricted contact tools is presented in the following.

According to Fig. 4 experiments are carried out with Ti6Al4V. The tests were conducted without metalworking fluid and with metalworking fluid pressure $p=30$ bar. Three different cutting speeds ($v_c = 38; 50$ and 75 m/min) with an uncut chip thickness of $h=0.1$ mm were considered. The experiments started with a restricted rake face length of $L_r=0.60$ mm and were successively shortened until tool breakage occurred. With each new rake face length, machining tests (three times) were carried out. The cutting force and the normal cutting force were measured. Figure 12 shows high-speed recordings during dry cutting at three different rake face lengths ($L_r=0.60; 0.30$ and 0.16 mm). Due to the experimental setup, the high-speed camera could not be aligned exactly perpendicular to the orthogonal cutting process. Furthermore, the segmentation of the chips is not visible because the magnification is not high enough. Nevertheless, analysis with the microscope show a typical serrated chip form within the observed process parameters. However, the high-speed recordings reveal how the chip forms with different restricted rake face lengths. With a rake face length of $L_r=0.6$ mm, the chip clearly curls below the rake face length. With a rake face length of $L_r=0.3$ mm, the restricted rake face is already close to the friction zone in the secondary shear zone of the cutting process. The camera recordings of $L_r=0.16$ mm show how the rake face length has fallen below the natural contact length. Through the

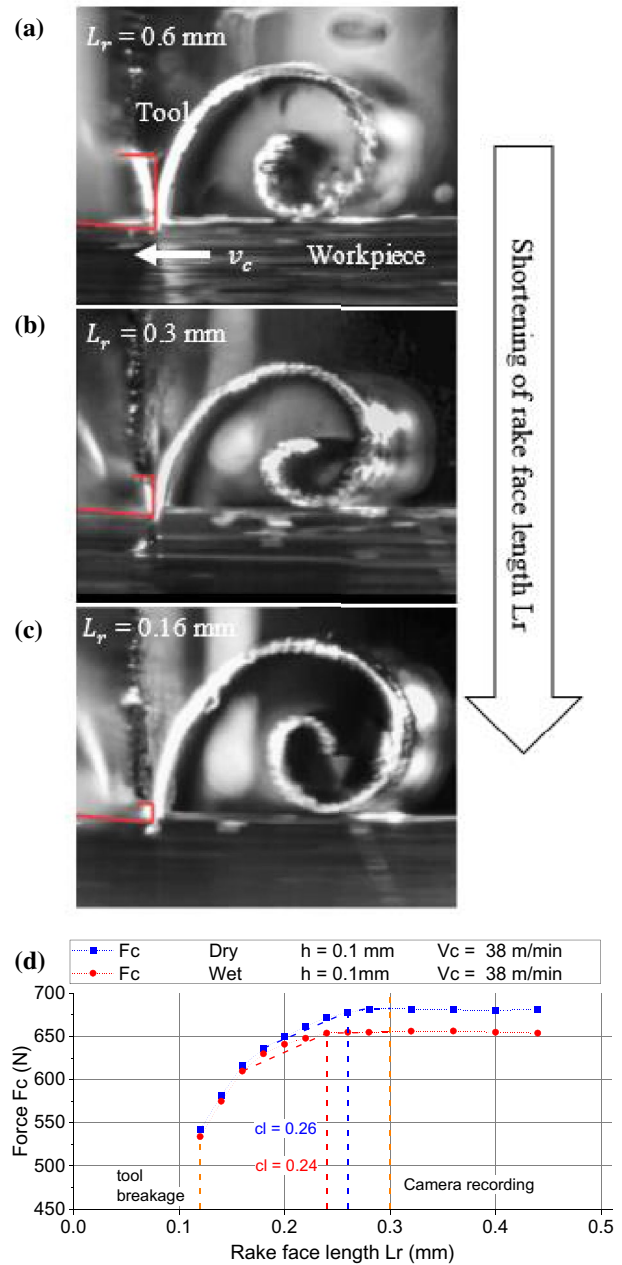


Fig. 12 a–c High speed images of orthogonal cutting of Ti6Al4V with $v_c=38$ m/min, $h=0.1$ mm and $b=3$ mm for dry process with different rake face lengths $L_r=0.6$ mm; 0.3 mm; 0.16 mm); **d** measured cutting forces (dry and wet $p=30$ bar); drop of cutting forces in dry and wet cutting (mean values of three processes)

high-speed camera recording, the drop in forces could be clearly assigned to falling below the natural contact length.

In general, it can be noticed that the cutting force and the cutting normal force are lower when using a metalworking fluid than in dry cutting. Cutting investigations with different materials show the same effect [16, 31]. This phenomenon was observed in all tests with different cutting speeds. The reasons for this are not fully clarified yet. Possible causes

could be that the application of metalworking fluid leads to less friction in the secondary shear zone. A reduced contact length due to the metalworking fluid could also be the reason. In Fig. 12, the cutting force characteristics for a cutting speed of $v_c = 38$ m/min in dry and wet cutting are shown. With continuous reduction of the rake face length, the cutting force begins to decrease after passing a certain rake face length. This also corresponds to studies in literature [21, 22]. However, the force measurements oscillate. Therefore, the average value from three repetition tests was used. For further assurance, chip curling before undergoing the natural contact length was ensured with the high-speed recordings up to a rake face length of $L_r = 0.3$ mm. When a falling force characteristic has been established, a tangent can be applied to the falling force values (criterion of falling forces (10%) over four restricted rake face length tests). The point of intersection between this tangent and the horizontal force characteristic indicates the contact length with the apparent contact area A_p . However, the tool-chip contact and thus the contact length fluctuates in this range, which is why the contact length determined from this must be regarded as a time-averaged value. The experiments show that the force characteristic in the dry cut decreases continuously from a rake face length of $L_r = 0.26$ mm. This indicates that the apparent contact area A_p has been undercut. The cutting force in wet cutting shows a similar characteristic up to a rake face length of 0.24 mm. By continuously reducing the rake face length the forces converge at a certain point. This can be explained by the fact that the metalworking fluid can only penetrate the contact zone between the chip and the rake face to a certain depth (apparent contact area A_p) due to the high temperatures and contact stresses existing there [33]. Nevertheless, slightly lower forces were measured in the wet section. At the rake face length $L_r = 0.12$ mm the tool broke.

Figure 13 shows the experimentally determined contact length with different cutting speeds. Because of the discontinuous chip formation process, the actual contact length varies. The results show that the contact length during machining of Ti6Al4V is shorter compared to other materials (Sects. 3.1 and 3.2). However, the results in dry cutting agree with results in literature where the contact length was determined by other methods under the same cutting parameters [13, 30]. Additionally, the results with laser textured tools (Sect. 3.1) show the same result for Ti6Al4V compared to AISI 4140+QT. An explanation for this effect could be the adiabatic shear chip formation when machining Ti6Al4V. In adiabatic shear chip formation, a constant change of sticking and shearing mechanism of the chip segments occurs. The low thermal conductivity of the material leads to an inhomogeneous heat distribution in the chip. The induced stress in tension and compression in the chip could result in this early curling and the related short contact

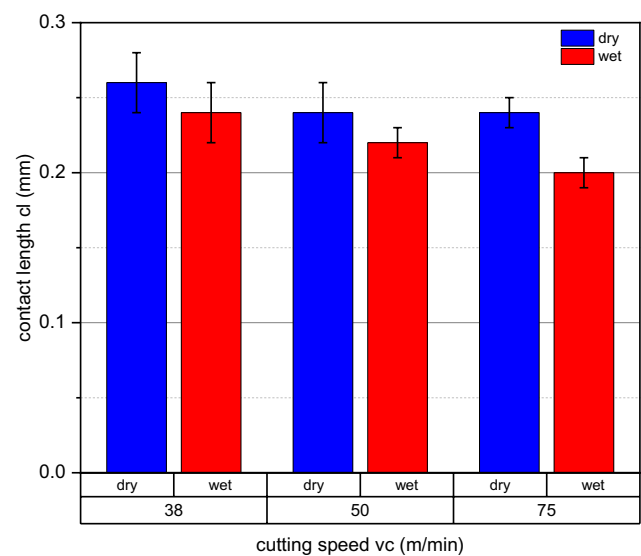


Fig. 13 Influence of cutting speed of contact length (apparent area A_p) in dry and wet cutting (mean value of three processes)

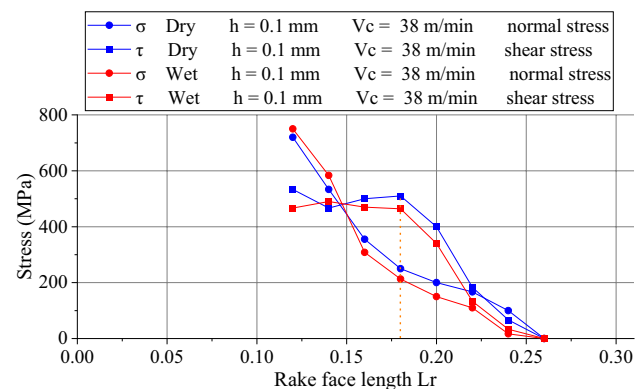


Fig. 14 Normal and shear stress on the rake face ($v_c = 38$ m/min, $h = 0.1$ mm and $b = 3$ mm, mean value of three processes)

length. Nevertheless, so far, no further research has been carried out on this issue. Higher cutting speeds show a slight decrease in contact length. The influence of a metalworking fluid is small and leads to a marginal reduction of the contact length. This was also determined with the method in Sect. 3.1.

According to Childs [1] and Özel et al. [28], the apparent contact area A_p and real contact area A_r differs due to the different contact and friction mechanisms. The real contact area and thus the real contact length can be determined by considering the stresses on the contact surface. By means of continuous rake face shortening, the force differences can be related to the respective rake face areas [22]. Figure 14 shows a calculated stress curve for $v_c = 38$ m/min. It can be seen, that the shear stresses assume a constant characteristic from a chip face length of $L_r = 0.18$ mm. This is in

Table 1 Comparison of the presented methods

	Micro-textured tools	High-speed recordings	Restricted contact length
Corresponding contact area A_p	$A_p = A_r$	$A_p > A_r$	$A_p > A_r$
Tool preparation methods	Laser-texturing	–	Grinding
Evaluation method	Microscope images	High-speed images	Force measurements
Add. setup for wet cutting	No	Camera protection	No
Minimum number of cuts	1	1	> 2
Additional process information	Chip thickness h'	Chip thickness h' , shear angle, built-up edges, local, velocity, local stresses [23]	Local stresses

accordance with [33]. From this, the real contact area A_r and the real contact length can be estimated. The results show, that the real contact area has not changed in machining Ti6Al4V comparing dry and wet conditions. Following Bahi et al. [33], a cooling lubricant in conventional machining (without any special microstructuring etc.) can mainly influence the sliding zone. If $A_p/A_r = 1$, the influence of the coolant on the contact length in the real contact surface becomes small.

4 Conclusions

This paper presents experimental investigations of the influence of a metalworking fluid on the contact properties between the chip and the tool rake face during the cutting process. Three different methods (micro-textured tools, high speed recordings, restricted contact length tools) are used to determine the natural contact length in orthogonal cutting. A material with continuous chip formation (AISI4140+QT) and a material with discontinuous chip formation (Ti6Al4V) were examined.

In general, a metalworking fluid leads to a reduced contact length in all tests. This can be attributed to the jet force and mechanical impact of the metal working fluid acting on the chip. Additionally, if a wetting of the rake face in the secondary cutting zone by the metalworking fluid occurs, an influence of the friction on the contact length can occur.

A comparison of the three methods is given in Table 1. When selecting the methods, it must first be taken into account that the contact lengths refer to different contact zones. With the method of microtextured tools, the contact zone is determined, in which the apparent contact area A_p corresponds approximately to the real contact area A_r . With the other two methods, on the other hand, the contact zone, in which the real contact area A_r is smaller than the apparent contact area A_p , is also taken into account. Thus, when statements about the real contact area have to be made, the method of laser-textured tools should be preferred. Another important aspect is the preparation time for the experiments. Regarding the tools, only for microtextured tools and tools

with restricted contact length a preparation is necessary. On the other hand, for wet cutting processes, additional measures must be carried out when high-speed images are recorded, to protect the equipment and enable the visibility of the cutting process. This fact makes the method the most time-consuming method in wet cutting, even though compared to the restricted contact length tool only one cut is necessary. However, the big advantage of the high speed-recordings are several additional process information, e.g., chip thickness, shear angle, local velocity vectors. Furthermore, local stresses can be calculated with the method given in [23].

In the end, it can be stated that the use of microtextured tools is an appropriate method to estimate the contact length in the zone $A_p = A_r$. When it comes to investigation of the contact length, where also the zone $A_p > A_r$ is included, two methods are applicable. While high-speed recordings compared to the restricted contact length tools are much more time-consuming when performing wet cutting processes, it has the advantage of additional process information.

Acknowledgements The authors appreciate the funding of this work within the Priority Program 2231 “Efficient cooling, lubrication and transportation—coupled mechanical and fluid-dynamical simulation methods for efficient production processes (FLUSIMPRO)” by the German Research Foundation (DFG)—Project Number 439904924, 439925537 and 439954775.

Funding Open Access funding enabled and organized by Projekt DEAL.

Open Access This article is licensed under a Creative Commons Attribution 4.0 International License, which permits use, sharing, adaptation, distribution and reproduction in any medium or format, as long as you give appropriate credit to the original author(s) and the source, provide a link to the Creative Commons licence, and indicate if changes were made. The images or other third party material in this article are included in the article’s Creative Commons licence, unless indicated otherwise in a credit line to the material. If material is not included in the article’s Creative Commons licence and your intended use is not permitted by statutory regulation or exceeds the permitted use, you will need to obtain permission directly from the copyright holder. To view a copy of this licence, visit <http://creativecommons.org/licenses/by/4.0/>.

References

1. Childs THC (2006) Friction modelling in metal cutting. *Wear* 260(3):S310–S318. <https://doi.org/10.1016/j.wear.2005.01.052>
2. Gad GS, Armarego EJA, Smith AJR (1992) Tool-chip contact length in orthogonal machining and its importance in tool temperature predictions. *Int J Prod Res* 30(3):485–501. <https://doi.org/10.1080/00207549208942907>
3. Özel T, Altan T (2000) Determination of workpiece flow stress and friction at the chip–tool contact for high-speed cutting. *Int J Mach Tools Manuf* 40(1):133–152. [https://doi.org/10.1016/S0890-6955\(99\)00051-6](https://doi.org/10.1016/S0890-6955(99)00051-6)
4. Puls H, Klocke F, Lung D (2012) A new experimental methodology to analyse the friction behaviour at the tool-chip interface in metal cutting. *Prod Eng Res Devel* 6(4–5):349–354. <https://doi.org/10.1007/s11740-012-0386-6>
5. Storchak M, Möhring H-C, Stehle T (2022) Improving the friction model for the simulation of cutting processes. *Tribol Int* 167(2):107376. <https://doi.org/10.1016/j.triboint.2021.107376>
6. Tsekhanov J, Storchak M (2015) Development of analytical model for orthogonal cutting. *Prod Eng Res Devel* 9(2):247–255. <https://doi.org/10.1007/s11740-014-0591-6>
7. Kato S, Yamaguchi K, Yamada M (1972) Stress distribution at the interface between tool and chip in machining. *J Eng Ind* 94(2):683–689. <https://doi.org/10.1115/1.3428229>
8. Childs THC, Mahdi MI, Barrow G (1989) On the stress distribution between the chip and tool during metal turning. *CIRP Ann* 38(1):55–58. [https://doi.org/10.1016/S0007-8506\(07\)62651-1](https://doi.org/10.1016/S0007-8506(07)62651-1)
9. Zorev NN (1963) Interrelationship between shear processes occurring along tool face and on shear plane in metal cutting. *ASME Int Res Prod Eng*. pp. 42–49
10. Finnie I, Shaw MC (1957) The friction process in metal cutting. *Trans ASME J Eng Ind* 79B:1649–1657
11. Böhm S, Ahsan A, Kröger J, Witte J (2020) Additive surface texturing of cutting tools using pulsed laser implantation with hard ceramic particles. *Prod Eng Res Devel* 14(5–6):733–742. <https://doi.org/10.1007/s11740-020-00984-7>
12. Sadik MI, Lindström B (1993) The role of tool-chip contact length in metal cutting. *J Mater Process Technol* 37(1–4):613–627. [https://doi.org/10.1016/0924-0136\(93\)90122-M](https://doi.org/10.1016/0924-0136(93)90122-M)
13. Iqbal SA, Mativenga PT, Sheikh MA (2009) A comparative study of the tool-chip contact length in turning of two engineering alloys for a wide range of cutting speeds. *Int J Adv Manuf Technol* 42(1–2):30–40. <https://doi.org/10.1007/s00170-008-1582-6>
14. Abukhshim NA, Mativenga PT, Sheikh MA (2004) An investigation of the tool-chip contact length and wear in high-speed turning of EN19 steel. *Proc Inst Mech Eng Part B J Eng Manuf* 218(8):889–903. <https://doi.org/10.1243/0954405041486064>
15. Sadik MI, Lindström B (1995) The effect of restricted contact length on tool performance. *J Mater Process Technol* 48(1–4):275–282. [https://doi.org/10.1016/0924-0136\(94\)01659-o](https://doi.org/10.1016/0924-0136(94)01659-o)
16. Courbon C, Kramar D, Krajnik P, Pusavec F, Rech J, Kopac J (2009) Investigation of machining performance in high-pressure jet assisted turning of Inconel 718: an experimental study. *Int J Mach Tools Manuf* 49(14):1114–1125. <https://doi.org/10.1016/j.ijmachtools.2009.07.010>
17. Lee EH, Shaffer BW (1951) The theory of plasticity applied to a problem of machining. *J Appl Mech* 18(4):405–413. <https://doi.org/10.1115/1.4010357>
18. Toropov A, Ko S-L (2003) Prediction of tool-chip contact length using a new slip-line solution for orthogonal cutting. *Int J Mach Tools Manuf* 43(12):1209–1215. [https://doi.org/10.1016/S0890-6955\(03\)00155-X](https://doi.org/10.1016/S0890-6955(03)00155-X)
19. Fatima A, Mativenga PT (2013) A review of tool-chip contact length models in machining and future direction for improvement. *Proc Inst Mech Eng Part B J Eng Manuf* 227(3):345–356. <https://doi.org/10.1177/0954405412470047>
20. Friedman MY, Lenz E (1970) Investigation of the tool-chip contact length in metal cutting. *Int J Mach Tool Des Res* 10(4):401–416. [https://doi.org/10.1016/0020-7357\(70\)90001-6](https://doi.org/10.1016/0020-7357(70)90001-6)
21. Heisel U, Kushner V, Storchak M (2012) Effect of machining conditions on specific tangential forces. *Prod Eng Res Devel* 6(6):621–629. <https://doi.org/10.1007/s11740-012-0417-3>
22. Ortiz-de-Zarate G, Madariaga A, Arrazola PJ, Childs THC (2021) A novel methodology to characterize tool-chip contact in metal cutting using partially restricted contact length tools. *CIRP Ann* 70(1):61–64. <https://doi.org/10.1016/j.cirp.2021.03.002>
23. Bergmann B, Grove T (2018) Basic principles for the design of cutting edge roundings. *CIRP Ann* 67(1):73–78. <https://doi.org/10.1016/j.cirp.2018.04.019>
24. Chiffre LD (1977) Mechanics of metal cutting and cutting fluid action. *Int J Mach Tool Des Res* 17(4):225–234. [https://doi.org/10.1016/0020-7357\(77\)90016-6](https://doi.org/10.1016/0020-7357(77)90016-6)
25. Chiffre LD (1981) Lubrication in cutting—critical review and experiments with restricted contact tools. *A S L E Trans* 24(3):340–344. <https://doi.org/10.1080/05698198108983030>
26. Varadarajan AS, Philip PK, Ramamoorthy B (2002) Investigations on hard turning with minimal cutting fluid application (HTMF) and its comparison with dry and wet turning. *Int J Mach Tools Manuf* 42(2):193–200. [https://doi.org/10.1016/S0890-6955\(01\)00119-5](https://doi.org/10.1016/S0890-6955(01)00119-5)
27. Dixit US, Sarma DK, Davim JP (2012) Environmentally friendly machining. Springer, Berlin. <https://doi.org/10.1007/978-1-4614-2308-9>
28. Özel T, Biermann D, Enomoto T, Mativenga P (2021) Structured and textured cutting tool surfaces for machining applications. *CIRP Ann* 70(2):495–518. <https://doi.org/10.1016/j.cirp.2021.05.006>
29. Patel KV, Jarosz K, Özel T (2021) Physics-based simulations of chip flow over micro-textured cutting tool in orthogonal cutting of alloy steel. *J Manuf Mater Process* 5(3):65. <https://doi.org/10.3390/jmmp5030065>
30. Pradhan S, Singh S, Prakash C, Królczyk G, Pramanik A, Prunco CI (2019) Investigation of machining characteristics of hard-to-machine Ti-6Al-4V-ELI alloy for biomedical applications. *J Market Res* 8(5):4849–4862. <https://doi.org/10.1016/j.jmrt.2019.08.033>
31. Denkena B, Krödel A, Ellersiek L (2022) Influence of metal working fluid on chip formation and mechanical loads in orthogonal cutting. *Int J Adv Manuf Technol* 118(9–10):3005–3013. <https://doi.org/10.1007/s00170-021-08164-2>
32. Denkena B, Biermann D (2014) Cutting edge geometries. *CIRP Ann* 63(2):631–653. <https://doi.org/10.1016/j.cirp.2014.05.009>
33. Bahi S, List G, Sutter G (2016) Modeling of friction along the tool-chip interface in Ti6Al4V alloy cutting. *Int J Adv Manuf Technol* 84(9–12):1821–1839. <https://doi.org/10.1007/s00170-015-7752-4>

Publisher's Note Springer Nature remains neutral with regard to jurisdictional claims in published maps and institutional affiliations.